Modeling of Turbulent Prandtl Number in Stationary and Homogeneous Stratified Turbulence

S. Hirabayashi and T. Sato
*Department of Ocean Technology, Policy, and Environment, University of Tokyo
5-1-5 Kashiwa-no-ha Kashiwa, 277-8563 Japan

Abstract – **The dependency of turbulent Prandtl number on the stratification stability was numerically investigated by means of direct numerical simulation of homogeneous and stratified turbulence in which the gradient Richardson number ranged from 0.05 to 0.15. It was found that the mixing efficiency was almost linearly correlated with the gradient Richardson number. By using this relation, turbulent Prandtl number was expressed by a simple model of linear function of the Richardson number. The proposed model of turbulent Prandtl number was implemented to large eddy simulation to find a better representation of the subgrid-scale diffusion coefficient for heat than the conventional constant model.**

I. Introduction

Turbulent Prandtl number (Pr_t) is one of the important parameters for characterizing the mixing process by turbulent eddies in stratified turbulence. In large eddy simulations (LES), turbulent diffusion of heat driven by subgrid-scale (SGS) eddies are often expressed by using SGS Prandtl number, which is commonly assumed to be constant in space and time. However, as suggested by Schumann and Gerz [1], Pr_t changes its value from 0.5 to 1.5 depending on the local gradient Richardson number (R_g) and it may become one of the reasons for discrepancies between the results of direct numerical simulations (DNS) and those of LES. It is expected that DNS can play an important role in developing a better model for LES by providing statistical data. For the purpose of modeling turbulence statistics, stationary and homogeneous turbulence is considered to be idealistic for removing the effect of spatial and temporal variations which makes physical characteristics of flow field much more complicated. Since stationary turbulence was achieved only by the trial and errors in the former studies, it had been difficult to investigate the dependency of statistics of stationary turbulence on primitive parameters such as Reynolds and Richardson numbers intensively.

In this study, homogeneous and stratified turbulence was numerically reproduced by a spectral method with forcing the mean vertical shear and the mean temperature gradient. The turbulence was kept statistically stationary by linear forcing developed recently by Hirabayashi [2] by controlling the forcing shear dynamically so as to achieve energy equilibrium under given energy dissipation and stratification.

II. Description of Numerical Methods

A. Governing Equations

In this section, numerical methods for direct numerical simulation of homogeneous and stratified turbulence for incompressible fluid are described. The governing equations are as follows: The continuity equation, the Navier-Stokes equations with the Boussinesq approximation, the heat transport equation. All the equations are expressed in a Lagrangian way for the mean vertical shear.

$$\frac{\partial u_j}{\partial x_j} = 0, \tag{1}$$

$$\frac{\partial u_i}{\partial t} + u_j \frac{\partial u_i}{\partial x_j} = -\frac{1}{\rho_0}\frac{\partial p}{\partial x_i} + \nu \frac{\partial^2 u_i}{\partial x_j^2} - g\beta T \delta_{i3} - u_i S_h \delta_{i1 i}, \tag{2}$$

$$\frac{\partial T}{\partial t} + u_j \frac{\partial T}{\partial x_j} = \kappa_T \frac{\partial^2 T}{\partial x_j^2} - u_j s \delta_{j3}, \tag{3}$$

where u_i is the velocity, p is the pressure, T is the temperature, ρ_0 is the standard density, g is the gravity acceleration, β is the coefficient of thermal expansion, ν is the kinematic viscosity, κ_T is the molecular thermal diffusivity, S_h is the mean vertical shear component, δ is the Kronecker delta and s is the mean vertical gradient of temperature. i, j = 1, 2 and 3 where 1 and 2 mean horizontal directions and 3 indicates vertical direction in the Cartesian coordinates. Repeated indices mean summation. S_h is determined dynamically so as to satisfy the energy equilibrium condition by the linear forcing method of Hirabayashi [2].

$$S_h = -\frac{\langle B \rangle + \langle \varepsilon \rangle}{\langle u_1 u_3 \rangle}. \tag{4}$$

where brackets indicate the volumetric average. B is the buoyancy flux and ε is the turbulent energy dissipation rate, defined respectively by

$$B = -g\beta T u_3, \tag{5}$$

$$\varepsilon = \nu \frac{\partial u_i}{\partial u_j}\left(\frac{\partial u_i}{\partial u_j} + \frac{\partial u_j}{\partial u_i}\right). \tag{6}$$

978-1-4244-5222-4/10/$26.00 ©2010 IEEE

B. Simulation method

Equations (1) to (4) were solved in a time-developing way by the finite difference method. The Poisson equation of pressure was solved iteratively to satisfy (1). The primitive variables were in staggered allocation, in which u_i are defined on the center of cell interfaces and the other variables are at the cell centers. For spatial differentiation, a 4th-order energy- and momentum-conserving scheme by Morinishi et al. [3] was adopted to the convection terms and a 2nd-order central difference scheme was adopted for the other terms. For time accuracy, a 3rd-order Adams-Bashforth method was used. The computational domain was a cube, the edge length of which was L.

C. Boundary and initial conditions

Based on the assumption of homogeneity, a normal periodic boundary condition was imposed for fluctuation components of u_i, p, and r on the horizontal boundaries. For the top and bottom boundaries, a shear-periodic boundary condition of Shumann [4] was adopted to take the effect of deformation into consideration.

The initial condition for u_i was given by the superposition of elementary waves, the amplitude and the direction of which were determined by random numbers to satisfy the following equations:

$$E(k) = 1.6\varepsilon_0^{2/3} k^{-5/3}, \tag{7}$$

$$k_j x_j = 0, \tag{8}$$

where (7) shows the prediction model of inertial subrange by the Kolmogorov hypothesis and (8) is the continuity equation in the wavenumber domain. The other components were set to be 0 at the initial state.

Table 1 Simulation conditions for DNS. $\eta = (\nu^3/\varepsilon_0)^{1/4}$ is the Kolmogorov scale, $L_O = (\varepsilon_0/N^3)^{1/2}$ is he Ozmidov scale, $\mathrm{Re}_L = (L/\eta)^{4/3}$ is the Reynolds number based on ε_0 and L, $\mathrm{Ri}_L = (L/L_O)^{4/3}$ is the Richardson number based on ε_0 and L, and $\mathrm{Re}_b = (L_O/\eta)^{4/3}$ is the buoyancy Reynolds number. The number of grids are 64x64x128 and 128^3 in Cases A1-A14 and Cases B1-B4, respectively.

Case	L	ε_0 (10^{-10})	N (10^{-3})	η (10^{-3})	L_O (m)	Re_L	Ri_L	Re_b
Unit	m	m^2/s^3	s^{-1}	m	m	-	-	-
A1			0.6		0.83		2.2	417
A2			0.65		0.74		2.6	355
A3			0.7		0.66		3.0	306
A4			0.75		0.60		3.4	267
A5			0.8		0.54		3.9	234
A6			0.9		0.45		4.9	185
A7		1.5	1.0	9.0	0.39	912	6.1	150
A8			1.05		0.36		6.7	136
A9			1.1		0.34		7.4	124
A10	1.5		1.2		0.29		8.8	104
A11			1.3		0.26		10.3	89
A12			1.4		0.23		11.9	77
A13			1.5		0.21		13.7	67
A14			1.6		0.19		15.6	59
B1			1.0		1.00		1.7	1000
B2		10	2.0	5.6	0.35	1717	6.9	250
B3			3.0		0.19		15.5	111
B4			4.0		0.13		27.5	63

D. Simulation cases

Table 1 shows the conditions of simulation cases. Input parameters are L, ε, and N.

III. MODELING OF TURBULENT PRANDTL NUMBER

From the results of the present DNS, volumetric and temporal average of parameters such as R_g, R_f, and Γ were obtained over the whole computational domain in the time period of $8 < t^* < 24$ in which turbulence was fully developed.

Fig. 1 shows the mixing efficiency, $\Gamma = B/\varepsilon$, plotted against gradient Richardson number, $R_g = N^2/S_h^2$. It is found that Γ is almost linear with R_g. It is also noted that the results of the present DNS agree well with those of experiments by Rohr et al. (1985) referred in Schumann and Gerz [1] although the experiments by Rohr and Van Atta [5] do not seem to fit to the DNS results.

Based on the idea that Γ should be 0 at $R_g = 0$, the following model for Γ is proposed:

$$\Gamma = \alpha R_g, \tag{9}$$

where $\alpha = 1.2$ is the proportional factor, which was obtained by the least square method from the present DNS results. Flux Richardson number, R_f, is then expressed by

$$R_f = \frac{\alpha R_g}{1 + \alpha R_g}. \tag{10}$$

Therefore, Pr_t was expressed by the following simple linear function.

$$\mathrm{Pr}_t = R_g + \frac{1}{\alpha}. \tag{11}$$

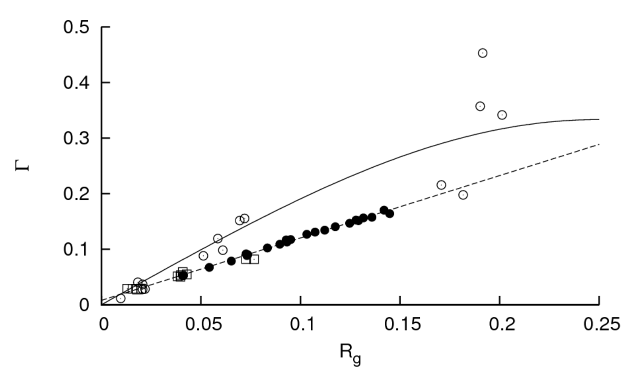

Figure 1. Mixing efficiency plotted against R_g. The data points are the present DNS results (closed circle), measurement by Rohr and Van Atta [5] (open square); and measurement by Rohr et al. (1985) reproduced from Fig.3 of Schumann and Gerz [1] (open circle). The lines are model fitted to DNS results (dashed) and model proposed by Baumert and Peters (2005) (solid).

Equation (11) was plotted in Fig. 2 together with the results of the present simulations. Prediction models by Baumert and Peters [6] and Schumann and Gerz [1] are also shown. It should be noted that the intercept of $1/\alpha = 0.84$ shows the Pr_t at $\mathrm{R_g} = 0$, which is larger than 0.72 suggested by Schumann and Gerz [1]. This discrepancy may be caused by the difference of Prandtl number for molecular diffusivity, which is set to be 1 in the present study while that for salt water is used in Schumann and Gerz [1]. Except for the intercept, all the models seem to express the present DNS results well in the range $0 < \mathrm{R_g} < 0.15$. Veneyagamoorthy and Stretch [7] suggested that Pr_t can be expresse by a linear model of $\mathrm{R_g}$ when $\mathrm{R_g} < 0.25$ and (11) is considered to be reasonable and used in the present study.

IV. Application to Large eddy simulations

A. Description of numerical methods in large eddy simulation

Equations (1) to (3) were low-pass filtered by the grid-scale (GS) filter as follows.

$$\frac{\partial \bar{u}_j}{\partial x_j} = 0, \tag{12}$$

$$\frac{\partial \bar{u}_i}{\partial t} + \bar{u}_j \frac{\partial \bar{u}_i}{\partial x_j} = -\frac{1}{\rho_0}\frac{\partial \bar{p}}{\partial x_i} + \frac{\partial}{\partial x_j}(\nu + \nu_{SGS})\frac{\partial \bar{u}_i}{\partial x_j} - g\beta \bar{T}\delta_{i3} - \bar{u}_i S_h \delta_{i1}, \tag{13}$$

$$\frac{\partial \bar{T}}{\partial t} + \bar{u}_j \frac{\partial \bar{T}}{\partial x_j} = \frac{\partial}{\partial x_j}(\kappa_T + \kappa_{SGS})\frac{\partial \bar{T}}{\partial x_j} - \bar{u}_j s \delta_{j3}, \tag{14}$$

where overbar indicates low-pass filtered component by the grid size. ν_{SGS} is the SGS (subgrid-scale) eddy viscosity, which is modeled by the following Smagorinsky model (1963):

$$\nu_{\mathrm{SGS}} = (C_S \Delta)^2 \left(2\bar{D}_{ij}\bar{D}_{ij}\right)^{1/2}, \tag{15}$$

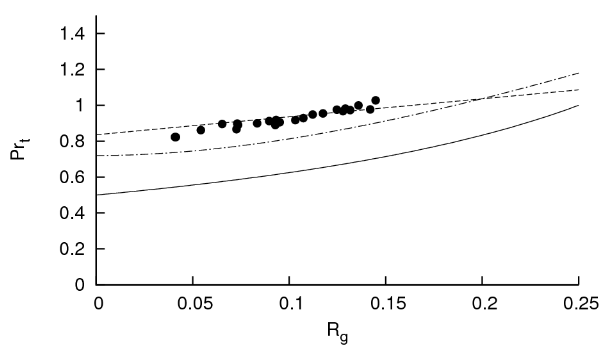

Figure 2. Turbulent Prandtl number, Pr_t plotted against $\mathrm{R_g}$. The closed circles are the present DNS results and the dashed line is a predicted line fitted to them. The solid line is the model by Baumert and Peters (2005) and the broken line is the model by Schumann and Gerz (1995).

where C_S is the Smagorinsky constant, which is set to be 0.173 by the theoretical prediction, Δ is the grid spacing, D_{ij} is the strain-rate tensor defined by

$$D_{ij} = \frac{1}{2}\left(\frac{\partial u_i}{\partial x_j} + \frac{\partial u_j}{\partial x_i}\right). \tag{16}$$

κ_{SGS} in (14) is the SGS eddy diffusivity and it is expressed from the analogy to the molecular diffusivity as

$$\kappa_{\mathrm{SGS}} = \frac{\nu_{\mathrm{SGS}}}{\mathrm{Pr_{SGS}}}, \tag{17}$$

where $\mathrm{Pr_{SGS}}$ is the SGS Prandtl number. When we assume that the turbulent Prandtl number, Pr_t, is homogeneous and it depends only on the stratification stability, Pr_t model can be substituted for $\mathrm{Pr_{SGS}}$. Therefore, $\mathrm{Pr_{SGS}}$ in (14) was calculated dynamically in the computation by using (11).

The simulation methods and boundary and initial conditions are the same as those adopted in the present DNS. The present LES were carried out for Cases B1 and B4 in Table 1. The grid number is 64^3 and 32^3 for each case. Additionally, LES with $\mathrm{Pr}_t = 1$ was also conducted in Case B1 64^3 for comparison.

B. Results and discussions

Table 2 is the turbulence statistics resulted from the present DNS and LES in Cases B1 and B4, where E is the turbulent kinetic energy, defined by

$$E = \frac{u_j u_j}{2}. \tag{18}$$

Turbulent kinetic energy dissipation rate, ε, for LES was obtained by the summation of GS and SGS components:

$$\varepsilon = \varepsilon_{\mathrm{GS}} + \varepsilon_{\mathrm{SGS}}, \tag{19}$$

$$\varepsilon_{\mathrm{GS}} = 2\nu \frac{\partial \bar{u}_i}{\partial x_j}\left(\frac{\partial \bar{u}_i}{\partial x_j} + \frac{\partial \bar{u}_j}{\partial x_i}\right), \tag{20}$$

$$\varepsilon_{\mathrm{GS}} = 2\nu_{\mathrm{SGS}} \frac{\partial \bar{u}_i}{\partial x_j}\left(\frac{\partial \bar{u}_i}{\partial x_j} + \frac{\partial \bar{u}_j}{\partial x_i}\right). \tag{21}$$

Table 2 Turbulence statistics resulted from the present DNS and LES. All the values are obtained by taking the temporal and volumetric average in $8 < t^* < 24$ over the simulation domain.

Case (×)	E^* 10^{-1}	ε^*	B^* 10^{-1}	$\mathrm{R_g}$ 10^{-1}	$\mathrm{R_f}$ 10^{-1}	Γ 10^{-1}
B1 DNS 128^3	6.01	0.94	0.53	0.41	0.50	0.53
B1 LES 64^3	6.00	0.92	0.60	0.45	0.56	0.61
B1 LES 64^3 $\mathrm{Pr}_t = 1$	6.76	0.90	0.64	0.50	0.60	0.63
B1 LES 32^3	7.00	0.86	0.70	0.59	0.66	0.70
B4 DNS 128^3	3.66	1.02	1.86	1.53	1.57	1.86
B4 LES 64^3	3.83	1.02	1.89	1.52	1.58	1.87
B4 LES 32^3	3.69	1.02	1.81	1.25	1.53	1.80

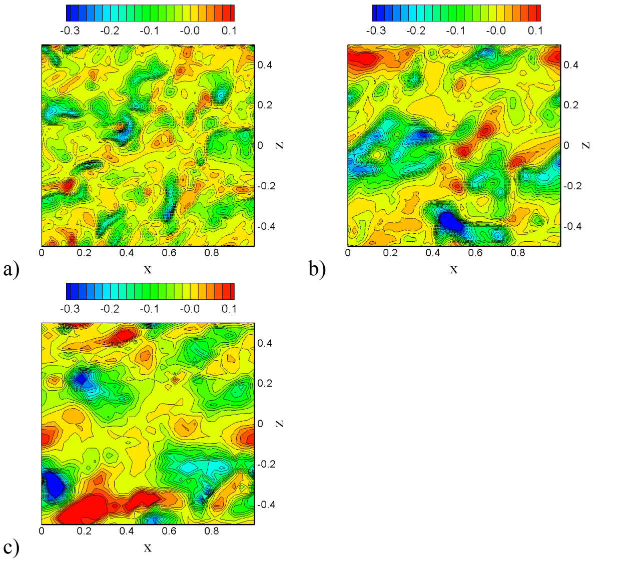

Figure 3 Instantaneous vertical cross section of vertical heat flux, wT, at $y^* = 0$ at $t^* = 24$ in Case B1, (a) DNS 128^3, (b) LES 64^3, and (c) LES 32^3.

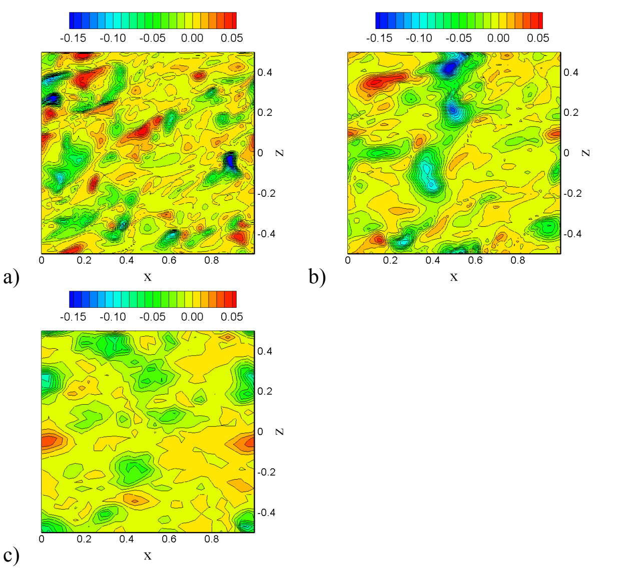

Figure 4 Instantaneous vertical cross section of vertical heat flux, wT, at $y^* = 0$ at $t^* = 24$ in Case B4, (a) DNS 128^3, (b) LES 64^3, and (c) LES 32^3.

It is found from Table 2 that results of LES with 64^3 grids show good agreements with DNS results in the both Cases B1 and B4 while coarse grid of 32^3 disagree with DNS in the range about 20 %. Between the same grid resolutions of 64^3 in Case B1, it can be seen that simulation with Pr_t model by (11) shows a better agreement than that with $\mathrm{Pr}_t = 1$. Since $\mathrm{R_g}$ in Case B1 LES 64^3 is 0.45, it is estimated that the averaged Pr_t by (11) was 0.88. On the other hand, Pr_t in Case B4 LES 64^3 was estimated to be 0.99.

Figs. 3 and 4 are the instantaneous vertical cross sections of vertical heat flux, wT, in the plane of $y^* = 0$ at $t^* = 24$ in Cases B3 and B4, respectively. There can be seen positive heat fluxes, which are corresponding to the counter-gradient (CG) heat fluxes. It is also noted that CG fluxes are attenuated by the decrease of grid resolution.

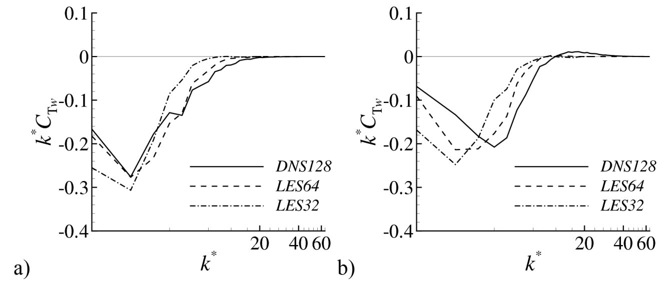

Figure 5 Cospectra of vertical heat flux, C_{Tw}, multiplied by k in Cases (a) B1 and (b) B4. Each spectrum was averaged in the time period of $12 < t^* < 24$.

Fig.5 shows the cospectra of vertical heat flux averaged in the time period of $12 < t^* < 24$. Because of temporal average, instantaneous CG fluxes in Case B1 vanishes and persistent CG fluxes can be seen only in Case B4. Apparently, LES does not express these heat fluxes properly, even though LES 64^3 grids can resolve them. Considering the agreement between DNS and LES 64^3, it is deduced that representation of small-scale, persistent CG fluxes by LES is not necessarily important in terms of turbulent statistics

V. CONCLUDING REMARKS

Turbulent Prandtl number in stationary and homogeneous stably stratified turbulence was modeled by direct numerical simulations. It was found that mixing efficiency was well expressed by proportional to gradient Richardson number. From this proportionality, a linear prediction model of turbulent Prandtl number was derived, which was supported by the previous studies. The proposed model was implemented to large eddy simulations and confirmed a better agreement with direct numerical simulation than conventional constant model. The persistent counter-gradient heat fluxes in the high wavenumber could not be found in LES results, suggesting that they may not be important for representation of turbulence statistics.

REFERENCES

[1] U. Schumann and T. Gerz, "Turbulent mixing in stably stratified shear flows," *J. Appl. Meteor.*, vol. 34, pp. 33-48, 1995.

[2] S. Hirabayashi, "Numerical study on vertical turbulent diffusivity in the ocean," Ph.D. thesis submitted to the University of Tokyo, 2009.

[3] Y. Morinishi, T. S. Luid, O. V. Vasilyev, and P. Moin, "Fully conservative higher order finite difference schemes for incompressible flow," *J. Comp. Phys.*, vol. 143, pp. 90-124, 1998.

[4] U. Schumann, "Algorithms for direct numerical simulation of shear-periodic turbulence," *in Proc. 9th Int. Conf. on Numerical Meth. in Fluid Dyn. Lecture Notes in Physics*, vol. 218, pp. 492-496, 1985.

[5] J. Rhor and C. Van Atta, "Mixing efficiency in stably stratified growing turbulence," J. Geophys. Res., vol. 92, pp. 5,481-5,483, 1987.

[6] H. Baumert and J. H. Simpson and J. Sündermann, "Marine turbulence," Cambridge University Press, Cambridge, pp. 630, 2005.

[7] S. K. Venayagamoorthy and D. D. Stretch, "On the turbulent Prandtl number in homogeneous stably stratified turbulence," J. Fluid Mech., vol. 644, pp. 359-368, 2010.